Void-Prism Ancillary Signal Update: Persistent Direction with Sub-1σ Null-Calibrated Evidence

Simulation Station Collaboration
E-mail: contact@simulationstation.example

Accepted 2026 February 12. Received 2026 February 12; in original form 2026 February 12

ABSTRACT

We present a compact status update of the standalone void-prism ancillary pipeline using five independent posterior seeds and three modified-gravity embeddings. The joint score is ΔLPD relative to an internal GR baseline. All seeds remain positive in all embeddings, with mean fitted-amplitude shifts +0.0423 (minimal), +0.0414 (slip-allowed), and +0.0490 (screening-allowed). A sign-only persistence test gives one-sided $p = 0.03125$ (1.86σ), but null-calibrated tests are not extreme: fast battery permutation/sign/data-placebo means are $p \sim 0.27$–0.55, map-level rotation/random-center placebos are $p \sim 0.47$–0.57, corresponding to roughly $|Z| \lesssim 0.6$ one-sided. Robustness remains limited: leave-one-out and leave-two-out all-positive fractions are zero for all embeddings, with nonpositive subset fractions 0.25 and 0.321. An external sky split (NGC versus SGC) is same-sign positive in all embeddings but amplitude-mismatched by factors ~ 15–16. The current channel is therefore directionally consistent but not decision-grade.

Key words: cosmology: observations – cosmology: theory – large-scale structure of Universe – gravitational lensing: weak

1 INTRODUCTION

Ancillary probes are useful for stress-testing the direction and channel localization of primary cosmological anomalies. Here we summarize the status of a void-conditioned prism observable based on the ratio

$$E_{\rm G}^{\rm void}(\ell) \propto \frac{C_{\kappa,v}(\ell)}{C_{\theta,v}(\ell)}, \tag{1}$$

constructed from Planck lensing, ACT/SDSS-derived velocity-proxy maps, and BOSS DR12 void catalog splits. The score reported throughout is

$$\Delta\mathrm{LPD}_{\rm vs\,GR} \equiv \mathrm{LPD}_{\rm model} - \mathrm{LPD}_{\rm GR}, \tag{2}$$

with GR treated as an internal baseline generated from the same background draws.

2 DATA PRODUCTS AND PIPELINE

The release includes a standalone implementation with: (i) theta-map construction, (ii) z/Rv-binned suite measurement with jackknife covariance, and (iii) joint posterior-predictive scoring. The bundled suite uses 8 blocks (4 redshift bins each split by median void radius), with 48-dimensional concatenated data vector and jackknife covariance from 603 regions. To support long runs, the current release includes partial-checkpoint/resume support for jackknife measurement and joint scoring.

The evidence update summarized here uses:

(i) explicit 5-seed × 3-embedding joint scoring with non-degenerate settings ($\eta_0 = 1.12$, $\eta_1 = -0.18$, $\alpha_{\rm env} = 0.25$, $\mu_{\rm P,high\text{-}z} = 1.05$);

(ii) a fast battery with 500 permutation/sign/data-placebo draws;

(iii) map-level placebo tests (rotation and mask-randomized centers, 64 draws per mode);

(iv) NGC/SGC split replication at max-draws 5000.

3 UPDATED MULTI-EMBEDDING RESULTS

Figure 1 shows per-seed ΔLPD values for each embedding in the explicit run. All seeds are positive in all embeddings, with modest seed-to-seed scatter. Screening-allowed gives the largest mean shift, while minimal and slip-allowed are close.

4 NULL-CALIBRATED TESTS

To test whether persistence indicates an isolated signal, we ran a fast battery over all five seeds and three embeddings:

- block-permutation null (misalignment null),
- block-sign null,
- data-placebo permutation null,
- leave-one and leave-two block drop tests,
- split consistency (low/high-z, small/large-R_v).

Figure 2 and Table 1 summarize the null tails. Permutation and data-placebo tails are typically $p \sim 0.27$–0.31; sign-null tails are $p \sim 0.51$–0.55. Under one-sided Gaussian mapping,

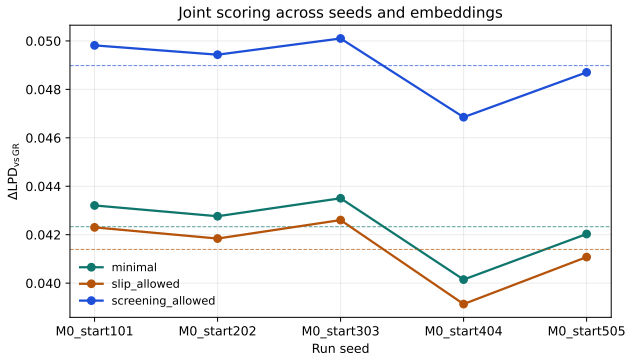

Figure 1. Per-seed fitted-amplitude ΔLPD values in the explicit 5-seed multi-embedding run. Dashed lines show embedding means.

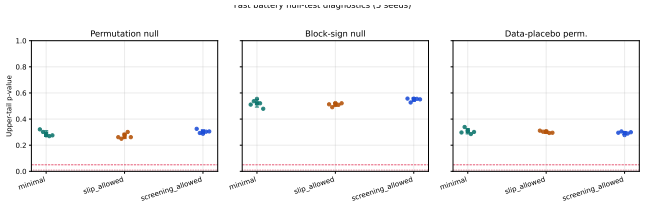

Figure 2. Fast-battery null diagnostics across five seeds for each embedding: permutation, block-sign, and data-placebo permutation tests. Horizontal red lines mark reference levels 0.05 and 0.01.

Table 1. Mean upper-tail null p-values by embedding (five seeds).

Embedding	Perm	Sign	Data-placebo	Rotate	Random-mask
minimal	0.289	0.521	0.307	0.471	0.551
slip_allowed	0.271	0.511	0.302	0.486	0.569
screening_allowed	0.303	0.549	0.293	0.471	0.511

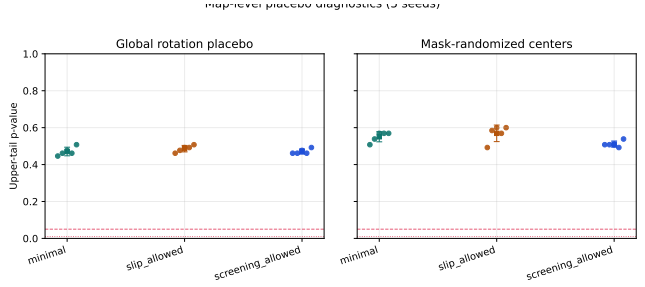

Figure 3. Map-level placebo diagnostics (global rotations and mask-randomized centers). Mean tails remain non-extreme for all embeddings.

this corresponds to approximately $|Z| \lesssim 0.6$. Map-level placebos (Figure 3) are also non-extreme.

5 ROBUSTNESS AND SPLIT REPLICATION

Figure 4 shows two robustness diagnostics. All embeddings keep positive low/high-z and small/large-R_v split means,

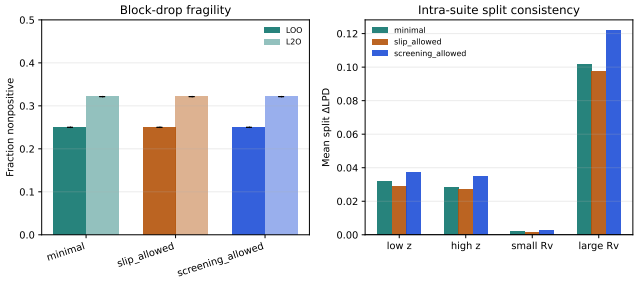

Figure 4. Robustness diagnostics. Left: fraction of nonpositive block-drop subsets (LOO and L2O). Right: intra-suite split means.

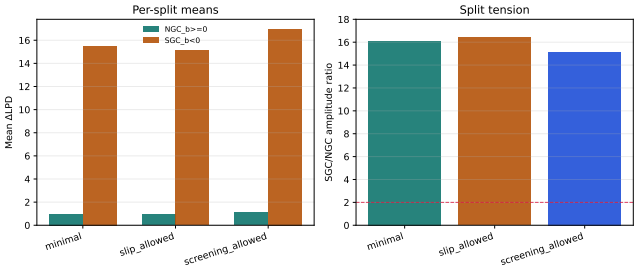

Figure 5. NGC/SGC split replication. Left: per-split means. Right: amplitude ratio (SGC/NGC), with dashed line at factor 2.

Table 2. Split replication mean ΔLPD and SGC/NGC amplitude ratio.

Embedding	NGC mean	SGC mean	Ratio
minimal	+0.964	+15.519	16.10
slip_allowed	+0.922	+15.126	16.41
screening_allowed	+1.121	+16.962	15.13

but block-drop stability is weak: the fraction of nonpositive subsets is 0.25 for leave-one-out and 0.321 for leave-two-out (all embeddings). The worst leave-two-out pair is identical in all runs: `zbin0_small_z0.200-0.360` plus `zbin1_small_z0.360-0.480`.

External split replication (Figure 5, Table 2) is same-sign positive but strongly amplitude-mismatched: SGC/NGC ratios are $\sim$ 15–16 in all embeddings.

6 CONCLUSION

The current status is:

(i) **Directional persistence:** all seeds are positive in all tested embeddings.
(ii) **Weak null-calibrated significance:** null tails correspond to about sub-1σ evidence.
(iii) **Structural fragility:** block-drop tests and NGC/SGC amplitude mismatch indicate incomplete robustness.

Therefore, the void-prism channel remains useful as a directional cross-check, but not yet as a standalone discriminator.

The data currently favor persistence in sign, while a fluke or residual systematic interpretation remains viable.

DATA AVAILABILITY

All artifacts used here are in-repo under: `artifacts/ancillary/void/void_prism_joint_explicit_multiembed_20260212_001503UTC/`, `outputs/void_prism_signal_battery_l2o_placebo_20260212_rerun/`, `outputs/void_prism_map_placebo_20260212_64x2/`, and `outputs/void_prism_split_replication_20260212_5000/`.

ACKNOWLEDGEMENTS

This manuscript was generated from the public repository release of the void-prism ancillary pipeline.

REFERENCES

Planck Collaboration et al., 2020, A&A, 641, A8
Aiola S. et al., 2020, JCAP, 12, 047
Mao Q. et al., 2017, MNRAS, 466, 1042

This paper has been typeset from a TEX/LATEX file prepared by the author.